RSC Advances

PAPER

View Article Online
View Journal | View Issue

Cite this: *RSC Adv.*, 2020, **10**, 29668

Amphiphilic poly(caprolactone-*b*-*N*-hydroxyethyl acrylamide) micelles for controlled drug delivery

Shuangxia Wu,[a] Fengjie Geng,[a] Suqin He,[ab] Wentao Liu, *[a] Hao Liu,*[a] Miaoming Huang[a] and Chengshen Zhu[a]

To increase the bioavailability and water solubility of hydrophobic medicine, an amphiphilic block copolymer, polycaprolactone-*block*-polyhydroxyethyl acrylamide (PCL-*b*-PHEAA), was synthesized. The copolymer can self-assemble into micelles by dialysis. The micelles were characterized by the Tyndall effect, static drop method, fluorescence spectrometry, dynamic light scattering, scanning electron microscopy and transmission electron microscopy. Ibuprofen was encapsulated inside the micelles by dialysis as a model medicine. The results show that the amphiphilic copolymer forms a uniform micelle system, with spherical micelles dispersed well in solution which have a low critical micelle concentration. In addition, the system shows good amphipathic behavior. Average particle size of a micelle is 104 nm, which increases a lot after drug loading and standing for half a month. In the first few hours, the cumulative release of the drug increases gradually; the rate of increase in the first ten hours is faster, then reaching a plateau which tends to be flat finally. It is similar under two different pH conditions. This biocompatible, biodegradable amphiphilic block copolymer has potential applications in the biomedical field.

Received 15th February 2020
Accepted 20th July 2020

DOI: 10.1039/d0ra01473g

rsc.li/rsc-advances

1. Introduction

Amphiphilic block copolymers, a research focus of nanomaterials, can self-assemble into nanoaggregates in selective solvents, which is commonly used to load hydrophobic drugs, genes, and proteins and for biological imaging.[1–3] When used as drug carriers, drug-loaded micelles self-assembled can increase the solubility of hydrophobic drugs such as ibuprofen, paclitaxel, and doxorubicin,[4–8] reduce side effects and prolong drug half-life. Zhao's group first prepared photosensitive micelles, and polyethylene glycol-*b*-poly(*o*-nitrobenzyl methacrylate) block copolymer was synthesized by atom transfer radical polymerization (ATRP), which self-assembled into micelles in aqueous solution. Nile red was loaded in the block copolymer micelles and it was shown that with this type of block copolymer micelles undergoing fast photoinduced disintegration of the micelle core, light-triggered burst release of loaded hydrophobic guest molecules in aqueous solution could be achieved.[9] Bae *et al.* designed and prepared functional poly(ethylene glycol)–poly(amino acid) block copolymers. The polymeric micelles feature a spherical sub-100 nm core–shell structure in which anticancer drugs are loaded avoiding undesirable interactions *in vivo*. Studies showed both controlled drug release and targeted delivery features of micelles reduced toxicity and improved efficacy significantly.[10] To date, though there are many studies on amphiphilic block copolymers, there are still many areas that have not been fully developed, so exploring new synthetic methods and designing new, specific functional block copolymers are also highlighted. Many hydrophobic segments have been used to fabricate amphiphilic block copolymers, *e.g.* *t*-butyl acrylate,[11] *n*-butyl acrylate,[12] poly(styrene),[13] polycaprolactone (PCL)[14–16] *etc.*

PCL is a linear hydrophobic polymer obtained by ring-opening polymerization of ε-caprolactone. It is reported that PCL has a higher permeability to many drugs, lower inflammatory response in living organisms, and less effect on the immune function of the body.[17] Recent studies on PCL have focused on the relationship between structure and properties.[18] Various pH-sensitive, temperature-sensitive, and nanoparticle polymers associated with PCL have since been fabricated. Cao *et al.* synthesized an ABA-type polymer, PCL-APS-PCL, which is spherical with a particle size of about 100 nm. This kind of polymer has a lower critical micelle concentration and it is a potential drug carrier.[16] Li *et al.* prepared a triblock copolymer, PEG-*b*-PCL-*b*-PDMAEMA-*g*-PC, with pH responsiveness, fluorescence and amphiphilicity, by ring-opening polymerization, ATRP and click reaction. The controlled release of DOX-loaded nanoparticles between cells was investigated.[19] Huang *et al.* successfully synthesized multifunctional polyelectrolyte CS/HA-*g*-PCL composite nanoparticles. In the gastrointestinal system, the nanoparticles can overcome the poor solubility of

[a]*School of Materials Science and Engineering, Zhengzhou University, Zhengzhou, Henan, 450001, PR China. E-mail: wtliu@zzu.edu.cn*

[b]*Henan Key Laboratory of Advanced Nylon Materials and Application, Zhengzhou University, Zhengzhou, 450001, PR China*

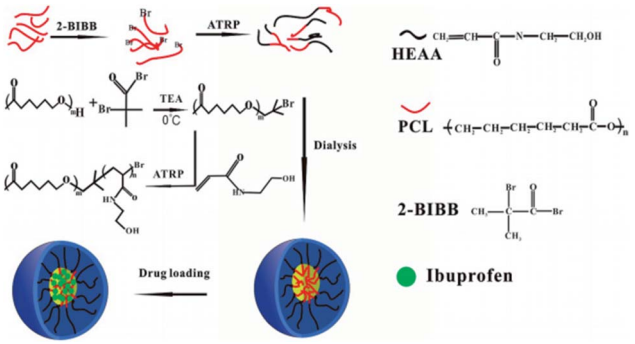

Fig. 1 Schematic diagram of synthesis process and drug loading of PCL-*b*-PHEAA.

hydrophobic drugs and enhance their transport.[20] PCL self-assembled into pH-responsive or temperature-responsive nanoaggregate in aqueous solution that can be used to deliver anticancer drugs and siRNA.[21,22] Despite that, there is still much potential for research into the preparation of PCL as a drug carrier.

Hydroxyethyl acrylamide (HEAA) is a hydrophilic polymer. It is usually used in biological, biomedical, and surface chemistry, and electrochemistry. The unique properties of HEAA, such as good flexibility, solubility and biocompatibility in water and organic solvents, make it useful as a polymeric carrier. Compared to polycarboxylic acids and trimethyl ethyl lactone polysulfonate, PHEAA has long-term biocompatibility and durability, which mean that it can be used as an alternative material for biomedical applications.[23–26] Amphiphilic block copolymer combining PCL and PHEAA shows good biocompatibility, bioavailability and hydrophilicity, and can self-assemble in selective solvents or aqueous solution to form a specific structure that can be used as a carrier for polymer drugs and drug release.

In this paper, the initiator PCL-Br was synthesized using PCL and 2-bromoisobutyryl bromide (BIBB), which was applied to initiate the polymerization of HEAA to get a new amphiphilic block copolymer, PCL-*b*-PHEAA.[27] A schematic diagram of the synthesis process is depicted in Fig. 1. The ratio of hydrophobic chains to hydrophilic chains was adjusted to obtain PCL_m-*b*-$PHEAA_n$ with different degree of polymerization, where *m* and *n* represent the degree of polymerization of PCL and PHEAA, respectively. Moreover, the drug loading performance of self-assembled spherical micelles was investigated.

2. Experimental

2.1 Materials

Materials included PCL (M_n = 10 000, Sigma-Aldrich), BIBB (analytically pure, Aladdin), triethylamine (TEA, analytically pure, Tianjin Chemical Reagent no. 1), HEAA (TCI), aluminum oxide (Al_2O_3, Tianjin Kemiou Chemical Reagent Co. Ltd), ibuprofen (IBU, Aladdin), cuprous bromide (CuBr, analytically pure, Sinopharm Group Chemical Reagent Co. Ltd), sodium bicarbonate ($NaHCO_3$, analytically pure, Tianjin Kemiou Chemical Reagent Co. Ltd), sodium chloride (NaCl, analytically pure, Tianjin Kemiou Chemical Reagent Co. Ltd), anhydrous magnesium sulfate ($MgSO_4$, analytically pure, Tianjin Kemiou Chemical Reagent Co. Ltd), methylene chloride (CH_2Cl_2, analytically pure, Yantai Shuangshuang Chemical Co. Ltd), methanol (CH_3OH, analytically pure, Yantai Shuangshuang Chemical Co. Ltd) and isopropanol ($(CH_3)_2CHOH$, analytically pure, Tianjin Shengao Chemical Reagent Co. Ltd).

2.2 Preparation of PCL-*b*-PHEAA amphiphilic block copolymer micelles

2.2.1 Preparation of PCL-Br. Reaction bottle was vacuumed and filled with nitrogen three times. Then PCL (2.5 g, 0.25 mol) was dissolved into 20 ml CH_2Cl_2 and kept stirring in nitrogen for 30 min. After PCL was dissolved entirely, 1.4 ml TEA was injected by a disposable syringe and stirred for 15 min. BIBB was added drop by drop (1.3 ml, diluted with 50 ml CH_2Cl_2). After being kept in an ice bath for 2 h and at room temperature for 24 h, the resulting solution was obtained.

All of the solution was filtered, and rinsed repeatedly with saturated $NaHCO_3$ and saturated NaCl. Then the resultant precipitate was dried with anhydrous $MgSO_4$ for 12 h. Finally, it was spin-steamed and precipitated in excess methanol. The precipitate was washed with distilled water and dried to constant weight at 40 °C in a vacuum drying oven to afford the initiator PCL-Br.

2.2.2 Preparation of copolymer PCL-*b*-PHEAA. Amphiphilic block copolymer was prepared by ATRP at 45 °C, in which PCL-Br was used as initiator, HEAA as the hydrophilic segment, and CuBr/2,2-bipyridine as the catalytic system.

PCL-Br (1.75 g) was dissolved in 15 ml of DMF with stirring in nitrogen until it dissolved entirely. Then 0.02 mmol CuBr, 0.4 mmol 2,2-bipyridine, and 40 mmol HEAA were added into the solution in turn. The reaction was kept at 24 °C for 24 h. After being vacuumed and filled with nitrogen, the reaction solution was passed through a neutral alumina column to remove CuBr using CH_2Cl_2 as the eluent, and the CH_2Cl_2 in the reaction liquid was removed by a rotary evaporator. Finally, the solution was precipitated in isopropanol to obtain a white solid powder, which was vacuum-dried to constant weight at 40 °C. The copolymer was denoted in an abbreviated form, namely PCL_m-*b*-$PHEAA_n$, where *m* and *n* represent the degree of polymerization.

2.2.3 Preparation of nanomicelles. 10 mg of PCL-*b*-PHEAA was dissolved in 2 ml of THF (tetrahydrofuran), then 8 ml of ultrapure water was added drop by drop. After that the solution changed from colorless and transparent to milky white. The solution was transferred to a dialysis bag (WMCO = 3500) with a large amount of ultrapure water. In this process, the ultrapure water was replaced periodically to ensure the complete removal of THF and promote the self-assembly of the polymer chains. After dialyzing for 48 h, a milky white micelle solution was obtained.

2.3 Preparation of drug-loaded PCL-*b*-PHEAA

10 mg of copolymer and 2 mg of IBU were dissolved in 10 ml of THF to obtain a homogeneous solution. Then the solution was

transferred into a dialysis bag with a large amount of ultrapure water for 24 h to remove THF completely. IBU was encased during the assembly process leading to drug-loaded micelles.

2.4 Determining ibuprofen release kinetics at different pHs

Buffer solutions of different pH were prepared, and the drug-loaded micelles placed in the buffer solution. The solution was put in a constant temperature water bath at 37 °C and shaken. Then, a certain amount of release medium was removed at regular intervals and the same amount of buffer solution added at the same time. An ultraviolet spectrophotometer was used to obtain the absorbance at the maximum absorption wavelength. Finally, a standard curve was constructed.

2.5 Characterization

The Tyndall effect was used to determine qualitatively the formation of micelles in the solution. To confirm quantitatively the formation of micelles self-assembled from PCL-*b*-PHEAA, the emission of a fluorescence probe was measured by a fluorescence spectrometer (QM40, PTI) based on selective partition of the fluorescence probe in hydrophobic phase against aqueous phase. Using pyrene as a probe, the fixed excitation wavelength is unchanged, scanning within a certain wavelength range, letting light of different wavelengths pass through the fluorescent solution to measure its fluorescence intensity, and the curve of excitation wavelength *versus* fluorescence intensity is the excitation spectrum. It has been reported that fluorescence spectra of pyrene solutions contain a vibrational band exhibiting high sensitivity to the polarity of the pyrene environment. As concentrations of PCL-*b*-PHEAA increased, the fluorescence intensity increased and the third peak shifted from 335 to 337 nm in the excitation spectra of pyrene. Therefore, the excitation wavelength was fixed at 337 nm to record the conformation of micelles.

The hydrophilic changes of PCL-*b*-PHEAA micellar solutions were characterized with static contact angle (JC2000C1) measurements.

The morphology of the micelles was observed using scanning electron microscopy (SEM) and transmission electron microscopy (TEM). Specimens for SEM observation were prepared by taking a small amount of the prepared micelle solution onto a clean silicon wafer, drying naturally and fixing it on the stage with conductive glue, spraying it with gold, and placing it under a scanning electron microscope (Phenom ProX). Specimens for TEM measurement were obtained by dropping about 10 μl of micellar solution uniformly after ultrasound treatment on carbon film-coated TEM grids. The grids were then allowed to air dry and specimens observed using an HT770 (Hitachi, Japan) microscope.[28]

After the micelle solution was uniformly dispersed, a small amount was taken in a clean cuvette and placed in a laser particle size analyzer (ZEN3690) to test the micellar particle size. The drug-loaded micelles were resuspended in PBS buffer at pH = 6.8 and pH = 7.4, and the release study was performed at 37 °C in an incubator shaker. At selected time intervals, the buffered solution outside the dialysis bag was removed for UV-visible (Cary 5000 UV-Vis) analysis and replaced with fresh buffer solution. IBU concentration was calculated based on the absorbance. Each experiment was repeated three times and the result was the mean value of three samples.

3. Results and discussion

When a beam of parallel light illuminates a colloidal solution, a path is clearly visible, which is a useful way to distinguish between solution and colloid (Fig. 2). This phenomenon indicates that the amphiphilic block copolymer self-assembles into a stable aggregate having a constant size in an aqueous solution. In addition to the hydrogen bond through the amide group, micelle formation is driven by the hydrophobic action of the PCL segment. The aggregates form a stable micelle system with a PCL block as the core and HEAA as the shell.

Fig. 3 displays the contact angle measurements. PCL is a hydrophobic polyester with a contact angle of 56.5° and the contact angle of PCL with a terminal *t*-butyl ester is about 70°.[19] PCL end groups in the raw material contain a hydrophilic hydroxyl group, so the contact angle is slightly lower. In aqueous solution, the contact angle of the block copolymer is about 31°, which is significantly reduced compared with that of PCL.

Fluorescence spectrometry was applied to study the critical micelle concentration. Considering that the pyrene molecule only has carbon and hydrogen and is very sensitive to environment changes, it is relatively hydrophobic and extremely suitable as a probe. When excited at 337 nm, pyrene shows five different levels of electronic vibration in the emission spectrum,

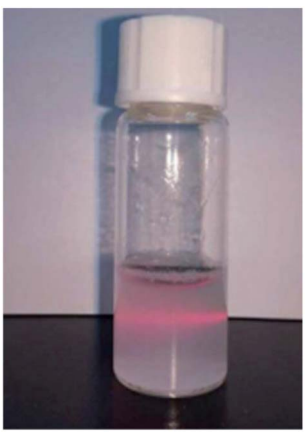

Fig. 2 Tyndall effect of PCL-*b*-PHEAA.

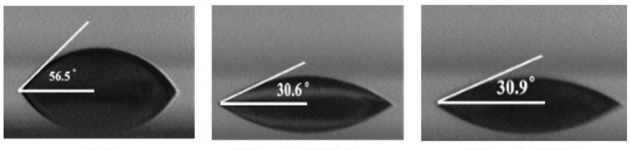

Fig. 3 Contact angle of PCL and copolymer.

and I_{383} and I_{372} correspond to the hydrophobic environment around the pyrene molecule. The red shift in the emission spectrum of pyrene indicates the enrichment of pyrene molecules from water to the inner core of micelles. The test result found that the emission peak at 372 nm was redshifted to 374.5 nm. The fluorescence intensity increases as the polymer concentration increases. Fig. 4 shows the ratio of intensities I_{383}/I_{372} plotted against logarithmic concentration of the diblock copolymer. As shown in Fig. 4(a), the ratio of fluorescence intensity I_{383}/I_{372} changes very little and is almost a straight line at low concentration of PCL_{109}-*b*-$PHEAA_{32}$. With the concentration increasing, the ratio of fluorescence intensity increases rapidly, representing the formation of micelles. With further increasing of concentration, there are no significant changes. The intersection of the two tangents is the inflection point: −2.79. The calculation revealed that the critical micelle concentration of the block copolymer PCL_{109}-*b*-$PHEAA_{32}$ is 1.62 μg ml^{-1}. For the copolymer PCL_{109}-*b*-$PHEAA_{14}$, an *S*-shaped curve is observed and the value at the intersection is −1.915 as shown in Fig. 4(b). Accordingly, the critical micelle concentration of the block copolymer PCL_{109}-*b*-$PHEAA_{14}$ is 12.2 μg ml^{-1}. This is almost consistent with the critical micelle concentration value of a PCL-based block copolymer reported in the literature.[29,30] The lower the critical micelle concentration, the more stable and easier to form are the micelles. The amphiphilic block copolymer shows excellent stability in aqueous solution. Due to the low body fluid concentration of the human body, such micelles can exist stably in the biological setting of body, and thereby can be used in drug delivery.

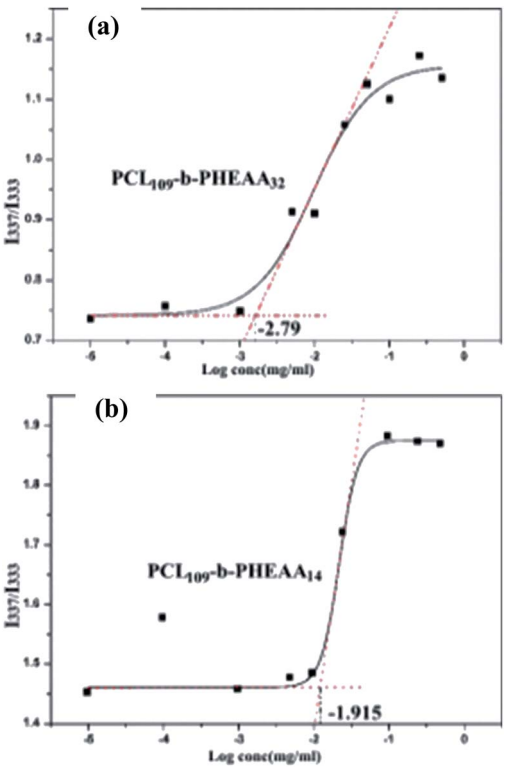

Fig. 4 The relationship between the fluorescence intensity ratio and the logarithm of micelle solution concentration of PCL-*b*-PHEAA at room temperature: (a) PCL_{109}-*b*-$PHEAA_{32}$; (b) PCL_{109}-*b*-$PHEAA_{14}$.

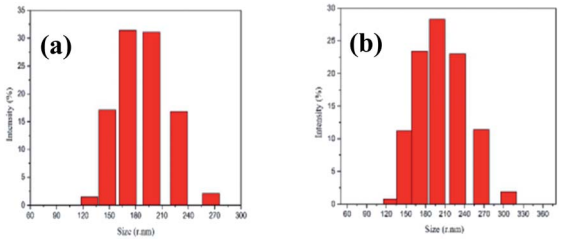

Fig. 5 The particle size distribution of the PCL-*b*-PHEAA copolymer micelles: (a) PCL_{109}-*b*-$PHEAA_{32}$; (b) PCL_{109}-*b*-$PHEAA_{14}$.

The average particle size and distribution of micelles in solution were determined by laser particle size analysis at 25 °C. The different polymer micelle solutions were prepared at a concentration of 0.1 mg ml^{-1}.

Fig. 5 shows that both copolymers PCL_{109}-*b*-$PHEAA_{32}$ and PCL_{109}-*b*-$PHEAA_{14}$ exhibit a uniform monomodal distribution. The copolymer PCL_{109}-*b*-$PHEAA_{32}$ self-assembles into micelle aggregates in aqueous solution, for which the average diameter is 519 ± 30 nm, and the PDI is 0.404. The copolymer PCL_{109}-*b*-$PHEAA_{14}$ has an average micelle diameter of 490 ± 15 nm and PDI of 0.311 in aqueous solution. This indicates that the size of the micelles satisfies the basic requirements for a drug carrier, and the size distribution is narrow, which is suitable for drug loading.

Effects of pH values on the particle size were also studied. The PCL_{109}-*b*-$PHEAA_{14}$ copolymer was formulated into a solution of 0.07 mg ml^{-1} with different pH, and then the particle size and its distribution were studied. As shown in Table 1, the particle sizes of the PCL_{109}-*b*-$PHEAA_{14}$ micelles decrease from 512.5 to 453.5 nm with the pH increasing from 4.0 to 9.2, whereas the PDI does not change obviously. An explanation for this trend can be given as follows. Acidic conditions can provide more hydrogen ions, and the hydrophilic segments containing hydroxyl and amide bonds can form more hydrogen bonds. Under the strong hydrogen bonds, the shell of the micelle is subjected to strong electrostatic repulsion, and the molecular chain exhibits a relatively stretched conformation, leading to the larger diameter of the particles. With pH increasing, the hydrogen bonding and the electrostatic repulsion of the shell molecular chain become weaker, resulting in a coiled conformational state of the molecular chain and the smaller diameter of the particles. At pH < 4, hydroxyl and amide groups are protonated and so appear electrostatic repulsions. Therefore, for these experimental conditions an increase of micelle sizes is observed. While at high pH values, those repulsions disappear

Table 1 The variation of PCL_{109}-*b*-$PHEAA_{14}$ micelle size at different pH values

pH	Particle size (nm)	PDI
4.0	512.5 ± 20	0.241
6.8	495.6 ± 15	0.257
9.2	453.5 ± 20	0.262

and a contraction of micelle size is observed. These results clearly show the pH-responsive property of the PCL-*b*-PHEAA copolymer.

SEM images of PCL-*b*-PHEAA samples are given in Fig. 6(a) and (b), showing a sample of PCL_{109}-*b*-$PHEAA_{32}$ at different magnifications. And Fig. 6(c) and (d) show images of a sample of PCL_{109}-*b*-$PHEAA_{14}$ at different magnifications. It can be seen that the copolymers self-assemble into spherical micelles. The surface of the micelles is smooth and the shape is regular, but some of the micelles agglomerate, leading to an obvious increase of the diameter.

From Fig. 6(d), concave areas on part of the spherical surface can be clearly seen, which is mainly caused by the removal of THF during dialysis. When ultrapure water is added to the THF solution containing the copolymer, the copolymer starts to self-assemble. At this time, the interface between THF and water undergoes microphase separation, in which the hydrophilic segment expands, and the hydrophobic segment entangles and shrinks. Part of the THF would leave because there is a lot of ultrapure water in the dialysis system, and the solution becomes unstable. With THF being removed continuously, the micelles are not completely formed and small bubbles occur between the particles, which gather, run to the outer surface of the sphere and finally break, leading to the formation of the shallow concave areas.

Fig. 7 shows SEM images of PCL_{109}-*b*-$PHEAA_{14}$ copolymer micelles derived from different buffers. The micelles at pH = 4 do not keep the regular spherical shape any more, but aggregate irregularly as shown in Fig. 7(a)–(c). Fig. 7(d)–(f) show the micelles have a regular spherical profile at pH = 6.8, and relatively flat surface, and the surface of the sphere has a thin shell layer to form a core–shell structure. In addition, the micelles at pH = 6.8 have good dispersibility although some of the nano-sized particles agglomerate into aggregates. At pH = 9.2, the micelles partly collapse showing spherical or ellipsoidal shapes, as shown in Fig. 7(g) and (h).

There are many factors affecting the change of micelle morphology. When microphase separation occurs, a copolymer can self-assemble into various forms of nano-domain. A micelle is a kinetic stabilization system. According to the VH theory put forward by Vilgis and Halperin, the morphology of micelles depends on the balance of three free energies, namely the free energy of the micelle nucleus, the free energy of the interface and the free energy of the shell. The free energy of the micelles dominates for crystalline micelles.

Besides, the initial stage of micelle formation is driven by thermodynamics. When a crystalline block copolymer is in a selective solvent, segments in the micelle core are frozen temporarily due to crystallization. So it is difficult for molecules to achieve thermodynamic equilibrium through chain exchange in a short time for macromolecular aggregates and block copolymers. Since PCL has strong crystallinity and lower crystallization temperature, the spherical micelles formed by direct dialysis tend to be rod or sheet shapes driven by crystallization. In addition, pH around cancer cells is lower than that of the normal body fluid. As a drug carrier, micelles would break under acidic conditions, which is favorable for drug delivery and can be used as the drug carrier.

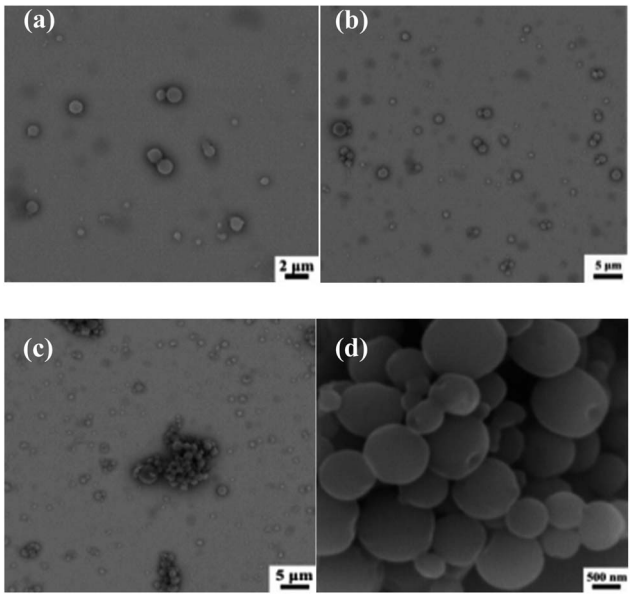

Fig. 6 SEM images of different copolymer micelles at a concentration of 1 mg ml^{-1}: (a and b) PCL_{109}-*b*-$PHEAA_{32}$; (c and d) PCL_{109}-*b*-$PHEAA_{14}$.

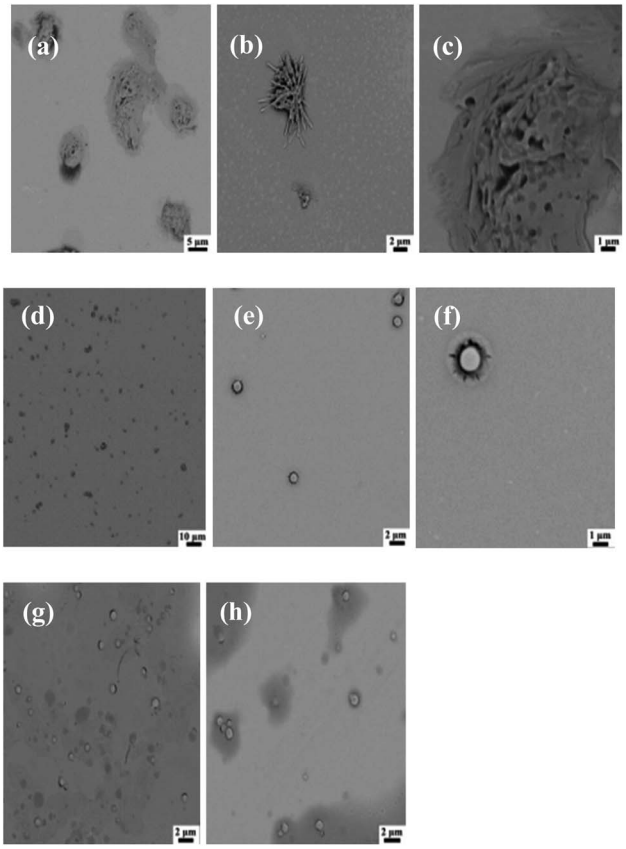

Fig. 7 SEM images of PCL_{109}-*b*-$PHEAA_{14}$ copolymer micelles derived from different buffers: (a–c) pH = 4.0; (d–f) pH = 6.8; (g and h) pH = 9.2.

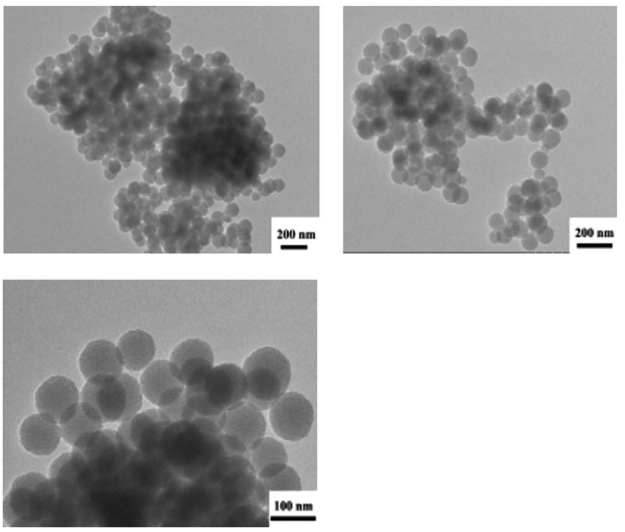

Fig. 8 TEM images of PCL_{109}-*b*-$PHEAA_{14}$ copolymer micelles self-assembled by dialysis in aqueous solution.

The spherical micelles self-assembled by dialysis in aqueous solution have good dispersibility and uniform size in aqueous solution as Fig. 8 shows. Average diameter of the micelle particles is 104 nm. The size was obviously smaller compared with the result of laser particle size analysis, which is mainly because the micelles measured by laser particle size analysis increase a lot after staying in the solution for a long time where a significant swelling reaction occurred.

Micelles were formed by dialysis, and then the hydrophobic drug IBU was wrapped into the core of the micelles by physical embedding. Fig. 9 shows that the diameter of the drug-loaded nanoparticles is 977 nm and PDI = 0.511. Compared with the empty micelles, the diameter and the PDI of the nanoparticles are significantly larger. One reason is that the drug enters into the core of the micelles by solubilization making the inner core become larger. Another reason is that in order to observe the stability of the micelles, the measurement was performed after 15 days. Although the solution is still milky white, the stability of the micelles decreases and some particles agglomerate, resulting in an increase of average particle size.

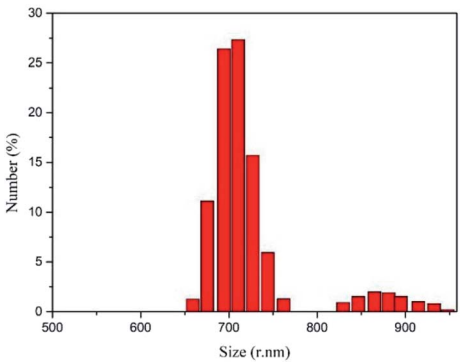

Fig. 9 Particle size distribution of PCL_{109}-*b*-$PHEAA_{14}$ drug-loaded nanoparticles.

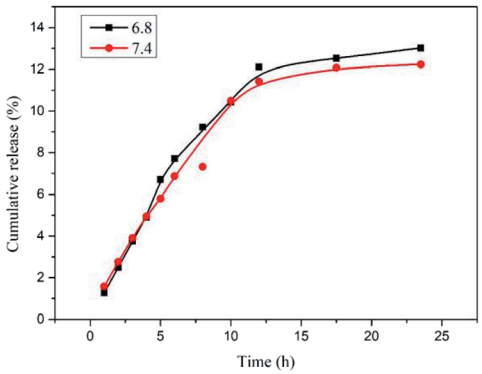

Fig. 10 Release profiles of IBU from PCL_{109}-*b*-$PHEAA_{14}$ drug-loaded nanoparticles at pH = 6.8 and pH = 7.4.

Fig. 10 shows the drug release profiles of drug-loaded nanoparticles in buffers with different pH. It can be seen from the figure that in the buffer solution of pH = 7.4, as time prolongs, the cumulative release of the drug increases gradually. The rate of increase in the first ten hours is faster, and then the rate of increase becomes slower which tends to be flat finally. The situation is similar when the pH is 6.8. The cumulative release of the drug is not much different between the two different pH values.

4. Conclusions

In summary, micelles of a new amphiphilic block copolymer, PCL-*b*-PHEAA, were synthesized in this work. The ratio of hydrophobic chains to hydrophilic chains was adjusted to obtain PCL_m-*b*-$PHEAA_n$ with different degree of polymerization, where *m* and *n* represent the degree of polymerization of PCL and PHEAA, respectively. Micelle properties, dispersibility, and drug loading efficiency of the micelles were measured. Related test results indicate that this new amphiphilic PCL-*b*-PHEAA block copolymer micelle has a lower critical micelle concentration, regular shape and good drug release performance. It will be a potential candidate for drug loading. However, the stability of this drug carrier is relatively poor, if storage time is too long. The size and performance may be changed. This requires us to conduct further research.

Conflicts of interest

There are no conflicts to declare.

Acknowledgements

This work is supported by the National Natural Science Foundation of China (grant no. U1504527) and Zhongyuan Science and Technology Innovation Leading Talents Project (194200510030).

References

1 P. L. Soo, L. Luo, D. Maysinger and A. Eisenberg, *Langmuir*, 2002, **18**, 9996–10004.

2 C. L. Gebhart and A. V. Kabanov, *J. Controlled Release*, 2001, **73**, 401–416.
3 S. W. Tan, H. J. Wang, K. H. Tu, H. L. Jiang and L. Q. Wang, *Chin. Chem. Lett.*, 2011, **22**, 1123–1126.
4 Y. Zhang, J. Chen, G. Zhang, J. Lu, H. Yan and K. Liu, *React. Funct. Polym.*, 2012, **72**, 359–364.
5 M. Hua, W. Yang, Q. Xue, M. Chen, X. Liu and C. Yang, *J. Chem.*, 2005, **63**, 631–636.
6 H. Han, Y. Li, J. Yuan and Q. Gao, *J. Polym. Sci.*, 2015, 1100–1106.
7 Y. Liu, J. Li, J. Ren, C. Lin and J. Leng, *Mater. Lett.*, 2014, **127**, 8–11.
8 R. Tang, W. Ji, D. Panus, R. N. Palumbo and C. Wang, *J. Controlled Release*, 2011, **151**, 18–27.
9 D. Han, X. Tong and Y. Zhao, *Macromolecules*, 2011, **44**, 437–439.
10 Y. Bae and K. Kataoka, *Adv. Drug Delivery Rev.*, 2009, **61**, 768–784.
11 P. Chmielarz, S. Park, A. Sobkowiak and K. Matyjaszewski, *Polymer*, 2016, **88**, 36–42.
12 X. Zhang, F. Boisson, O. Colombani, C. Chassenieux and B. Charleux, *Macromolecules*, 2014, **47**, 51–60.
13 A. A. Purchel, W. S. Boyle and T. M. Reineke, *Mol. Pharm.*, 2019, **16**, 4423–4435.
14 Z. Duan, L. Zhang, H. Wang, B. Han, B. Liu and I. Kim, *React. Funct. Polym.*, 2014, **82**, 47–51.
15 I. L. Diaz and L. D. Perez, *Colloid Polym. Sci.*, 2015, **293**, 913–923.
16 J. Cao, K.-M. Xiu, K. Zhu, Y.-W. Chen and X.-L. Luo, *J. Biomed. Mater. Res., Part A*, 2012, **100**, 2079–2087.
17 A. Kumari, S. K. Yadav and S. C. Yadav, *Colloids Surf., B*, 2010, **75**, 1–18.
18 D. Newman, E. Laredo, A. Bello and P. Dubois, *Macromolecules*, 2014, **47**, 2471–2478.
19 L. Li, B. Lu, Q. Fan, L. Wei, J. Wu, J. Hou, X. Guo and Z. Liu, *RSC Adv.*, 2016, **6**, 27102–27112.
20 P. Huang, C. Yang, J. Liu, W. Wang, S. Guo, J. Li, Y. Sun, H. Dong, L. Deng, J. Zhang, J. Liu and A. Dong, *J. Mater. Chem. B*, 2014, **2**, 4021–4033.
21 J. Fan, F. Zeng, S. Wu and X. Wang, *Biomacromolecules*, 2012, **13**, 4126–4137.
22 X.-B. Xiong, H. Uludag and A. Lavasanifar, *Biomaterials*, 2009, **30**, 242–253.
23 G. Li, H. Xue, G. Cheng, S. Chen, F. Zhang and S. Jiang, *J. Phys. Chem. B*, 2008, **112**, 15269–15274.
24 Z. Zhang, J. A. Finlay, L. Wang, Y. Gao, J. A. Callow, M. E. Callow and S. Jiang, *Langmuir*, 2009, **25**, 13516–13521.
25 Y. Chang, W.-J. Chang, Y.-J. Shih, T.-C. Wei and G.-H. Hsiue, *ACS Appl. Mater. Interfaces*, 2011, **3**, 1228–1237.
26 Y.-J. Shih and Y. Chang, *Langmuir*, 2010, **26**, 17286–17294.
27 F. Geng, H. Liu, Y. Liu, *et al.*, *Polym. Mater.: Sci. Eng.*, 2018, **034**(007), 20–24.
28 O. Vierrether, J. TerBush and C. Wisner, *Microsc. Microanal.*, 2016, **22**, 1914–1915.
29 W. H. Xie, W. P. Zhu and Z. Q. Shen, *Polymer*, 2007, **48**, 6791–6798.
30 Z. B. Li and B. H. Tan, *Mater. Sci. Eng., C*, 2014, **45**, 620–634.